Available online at www.sciencedirect.com

SciVerse ScienceDirect

Ceramics International 39 (2013) 917–923

CERAMICS INTERNATIONAL

www.elsevier.com/locate/ceramint

Electrochemical performance of cobalt-substituted lithium nickel oxides synthesized from lithium and nickel carbonates and cobalt oxide

Ho Rim[a], Hye Ryoung Park[b], Myoung Youp Song[c,*]

[a]ASE Korea, 494 Munbal-dong Paju-si Gyeonggi-do, 413-790, Republic of Korea
[b]School of Applied Chemical Engineering, Chonnam National University, 300 Yongbong-dong Buk-gu Gwangju, 500-757, Republic of Korea
[c]Division of Advanced Materials Engineering, Hydrogen & Fuel Cell Research Center, Engineering Research Institute, Chonbuk National University,664-14 Deogjindong 1Ga Deogjingu, 567 Baekje-daero Deokjin-gu Jeonju, 561-756, Republic of Korea

Received 22 May 2012; received in revised form 30 June 2012; accepted 1 July 2012
Available online 17 July 2012

Abstract

$LiNi_{1-y}Co_yO_2$ ($y=0.1$, 0.3 and 0.5) cathode materials were synthesized by a solid-state reaction method at different temperatures using Li_2CO_3 as a Li source, $NiCO_3$ as a Ni source, and Co_3O_4 as a Co source. The electrochemical properties of the synthesized samples were then investigated. Structures of the synthesized $LiNi_{1-y}Co_yO_2$ ($y=0.1$, 0.3 and 0.5) samples were analyzed, and microstructures of the samples were observed. Voltage vs. x in $Li_xNi_{1-y}Co_yO_2$ curves for the first and second charge–discharge cycles and intercalated and deintercalated Li quantity Δx were studied. $LiNi_{0.9}Co_{0.1}O_2$ synthesized at 800 °C had the largest first discharge capacity (152 mAh/g) and quite good cycling performance, with a discharge capacity of 146 mAh/g at $n=5$. It had a discharge capacity fading rate of 1.4 mAh/g/cycle.

Keywords: $LiNi_{1-y}Co_yO_2$; Solid-state reaction method; Voltage vs. x in $Li_xNi_{1-y}Co_yO_2$ curve; Cycling performance

1. Introduction

As cathode materials for lithium secondary batteries, transition metal oxides such as $LiCoO_2$ [1–5], $LiNiO_2$ [6–13], and $LiMn_2O_4$ [14–20] have been investigated by many researchers [21]. $LiMn_2O_4$ is relatively cheap and environment-friendly, but has poor cycling performance. $LiCoO_2$ has a large diffusivity and a high operating voltage, and it can be easily prepared. However, it has a disadvantage that it contains an expensive element, Co.

$LiNiO_2$ is a very promising cathode material because it has a large discharge capacity [22] and is relatively excellent from the viewpoints of economics and environment. However, because Li and Ni have similar ionic radii ($Li^+=0.72$ Å and $Ni^{2+}=0.69$ Å), the $LiNiO_2$ is practically obtained in the non-stoichiometric compositions, $Li_{1-y}Ni_{1+y}O_2$ [23,24], and the Ni^{2+} ions in the lithium planes obstruct the movement of the Li+ ions during charge and discharge [25,26].

By incorporating $LiCoO_2$ and $LiNiO_2$ phases into $LiNi_{1-y}Co_yO_2$ compositions, the shortcomings of $LiCoO_2$ and $LiNiO_2$ can be remedied because the presence of cobalt stabilizes the structure in a strictly two-dimensional fashion, thus favoring good reversibility of the intercalation and deintercalation reactions [25,27–39]. Rougier et al. [25] reported that the stabilization of the two-dimensional character of the structure by cobalt substitution in $LiNiO_2$ is correlated with an increase in the cell performance, due to the decrease in the amount of extra-nickel ions in the inter-slab space which impede the lithium diffusion. Kang et al. [39] investigated the structure and electrochemical properties of the $Li_xCo_yNi_{1-y}O_2$ ($y=0.1$, 0.3, 0.5, 0.7 and 1.0) system synthesized by a solid-state reaction with various starting materials to optimize the characteristics and synthetic conditions of

*Corresponding author. Tel.: +82 63 270 2379; fax: +82 63 270 2386.
E-mail address: songmy@jbnu.ac.kr (M. Youp Song).

0272-8842/$36.00
http://dx.doi.org/10.1016/j.ceramint.2012.07.006

the $Li_xCo_yNi_{1-y}O_2$. The first discharge capacities of $Li_xCo_yNi_{1-y}O_2$ were 60–180 mAh/g, depending on synthesis conditions.

Several methods have been reported for the synthesis of $LiNiO_2$ and $LiNi_{1-y}Co_yO_2$ such as the solid-state reaction method [40,41], the coprecipitation method [42], the sol–gel method [43], the ultrasonic spray pyrolysis method [44], the combustion method [11], and the emulsion method [45]. The solid-state reaction method was chosen in this work for its simplicity.

Researchers used different starting materials to synthesize $LiNi_{1-y}Co_yO_2$ by the solid-state reaction method [25,27–30,32–34,38,39,46]. $LiOH \cdot H_2O$ or Li_2CO_3, NiO or $NiCO_3$, and Co_3O_4 or $CoCO_3$ have been used as starting materials by some researchers [39,46] in order to synthesize $LiNi_{1-y}Co_yO_2$ by the solid-state reaction method.

In this work, $LiNi_{1-y}Co_yO_2$ ($y=0.1$, 0.3 and 0.5) cathode materials were synthesized by solid state reaction method at different temperatures using Li_2CO_3 as a source of Li, $NiCO_3$ as a source of Ni, and Co_3O_4 as a source of Co as starting materials. The electrochemical properties of the synthesized samples were then investigated. The structures of the synthesized $LiNi_{1-y}Co_yO_2$ ($y=0.1$, 0.3 and 0.5) were analyzed, and the microstructures of the samples were observed. Voltage vs. x in $Li_xNi_{1-y}Co_yO_2$ curves for the first and second charge–discharge cycles and intercalated and deintercalated Li quantity Δx were studied.

2. Experimental

Li_2CO_3, $NiCO_3$ and Co_3O_4 were used as starting materials in order to synthesize $LiNi_{1-y}Co_yO_2$ by the solid-state reaction method. All the starting materials (with the purity 99.9%) were purchased from Aldrich Co.

The experimental procedure for $LiNi_{1-y}Co_yO_2$ synthesis from Li_2CO_3, $NiCO_3$ and Co_3O_4 and subsequent characterization is given schematically in Fig. 1. The mixture of starting materials in the compositions of $Li_{1.1}Ni_{1-y}Co_yO_2$ ($y=0.1$, 0.3 and 0.5) was mixed sufficiently and pelletized. Excess Li_2CO_3 was added to compensate for the lithium evaporated during heat treatment and calcination. This pellet was heat-treated in air at 650 °C for 20 h. It was then ground, mixed, pelletized again and calcined at either 800 °C or 850 °C for 20 h. This pellet was cooled at a cooling rate of 50 °C/min, ground, mixed and pelletized again. It was then calcined again at either 800 °C or 850 °C for 20 h.

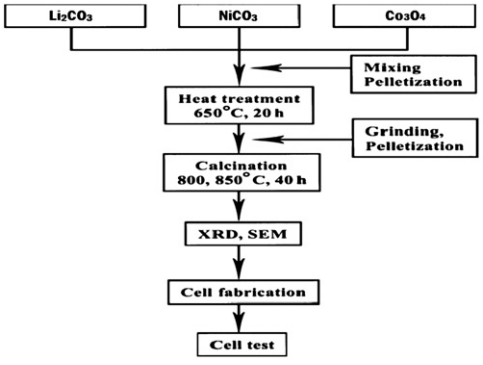

Fig. 1. Schematic of experimental procedure for $LiNi_{1-y}Co_yO_2$ synthesis from Li_2CO_3, $NiCO_3$ and Co_3O_4 and subsequent characterization.

The phase identification of the synthesized samples was carried out by X-Ray Diffraction (XRD) analysis using Cu K_α radiation (Mac-Science Co., Ltd.). The scanning rate was 16°/min and the scanning range of diffraction angle (2θ) is $10° \le 2\theta \le 70°$. The morphologies of the samples were observed using a scanning electron microscope (SEM).

Electrochemical cells consisted of $LiNi_{1-y}Co_yO_2$ as the positive electrode, Li foil as the negative electrode, and 1 M $LiPF_6$ in a 1:1 volume ratio mixture of ethylene carbonate (EC) and dimethyl carbonate (DMC) as the electrolyte. A Whatman glass-fiber was used as the separator. The cells were assembled in an argon-filled dry box. To fabricate the positive electrode, 89 wt% synthesized oxide, 10 wt% acetylene black, and 1 wt% Polytetrafluoroethylene (PTFE) binder were mixed in an agate mortar. By introducing Li metal, Whatman glass-fiber, positive electrode, and electrolyte, the cell was assembled. All the electrochemical tests were performed at room temperature with a potentiostatic/galvanostatic system (Mac-Pile system, Bio-Logic Co. Ltd.). The cells were cycled at a current density of 200 μA/cm^2 in a voltage range of 3.2–4.3 V.

3. Results and discussion

XRD patterns of $LiNi_{1-y}Co_yO_2$ ($y=0.1$, 0.3 and 0.5) powders calcined at 800 °C for 40 h using Li_2CO_3, $NiCO_3$ and Co_3O_4 as starting materials are shown in Fig. 2.

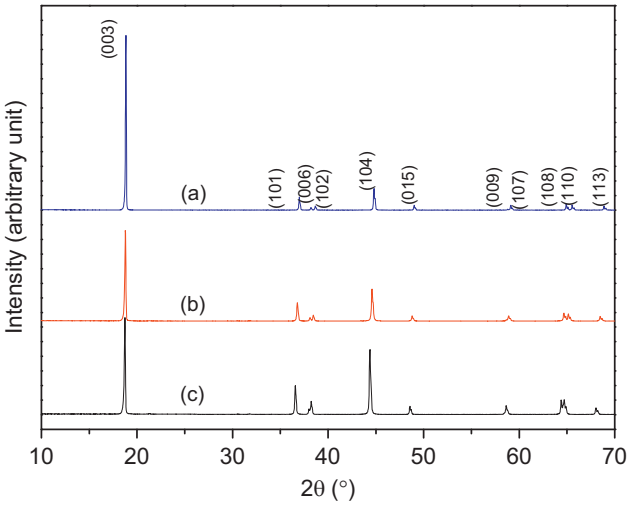

Fig. 2. XRD patterns of $LiNi_{1-y}Co_yO_2$ powders calcined at 800 °C for 40 h using Li_2CO_3, $NiCO_3$ and Co_3O_4 as starting materials; (a) $y=0.5$, (b) $y=0.3$, and (c) $y=0.1$.

The peaks are identified as corresponding to those of the $LiNiO_2$ phase, which has the α-$NaFeO_2$ structure with a space group of $R\bar{3}m$. XRD patterns of $LiNi_{1-y}Co_yO_2$ ($y=0.1$, 0.3 and 0.5) powders calcined at 850 °C for 40 h using Li_2CO_3, $NiCO_3$ and Co_3O_4 as starting materials showed XRD patterns very similar to these ones in Fig. 2 with no evidence of impurities.

SEM micrographs of $LiNi_{1-y}Co_yO_2$ synthesized from Li_2CO_3, $NiCO_3$ and Co_3O_4 at 800 °C; (a) $y=0.5$, (b) $y=0.3$, and (c) $y=0.1$, and at 850 °C; (d) $y=0.5$, (e) $y=0.3$, and (f) $y=0.1$ are shown in Fig. 3. When the particle sizes for samples synthesized at 800 °C are compared, the particle size increases very slightly as the Co content decreases, but the differences overall are quite small. When the particle sizes are compared for the samples synthesized at 850 °C, $LiNi_{0.5}Co_{0.5}O_2$ has the smallest particle size, followed in order by $LiNi_{0.9}Co_{0.1}O_2$ and $LiNi_{0.7}Co_{0.3}O_2$. For a given composition, the sample synthesized at 800 °C has smaller particle size than the sample synthesized at 850 °C. The particle sizes of all the samples except for $LiNi_{0.7}Co_{0.3}O_2$ synthesized at 850 °C are quite homogeneous, and the particles of all the samples are agglomerated.

Voltage vs. x in $Li_xNi_{1-y}Co_yO_2$ curves at a current density of 200 μA/cm^2 for the first charge–discharge cycle of $LiNi_{1-y}Co_yO_2$ synthesized at 800 °C; (a) $y=0.5$, (b) $y=0.3$, and (c) $y=0.1$, and at 850 °C; (d) $y=0.5$, (e) $y=0.3$, and (f) $y=0.1$ are shown in Fig. 4. Polarization is a change in potentials for deintercalation and intercalation of lithium atoms. The $LiNi_{1-y}Co_yO_2$ ($y=0.1$, 0.3 and 0.5) samples synthesized at 800 °C and $LiNi_{0.9}Co_{0.1}O_2$ synthesized at 850 °C exhibit quite small polarization. Of the $LiNi_{1-y}Co_yO_2$ ($y=0.1$, 0.3 and 0.5) synthesized at 800 °C, $LiNi_{0.9}Co_{0.1}O_2$ has the largest intercalated Li quantity Δx, followed by $LiNi_{0.7}Co_{0.3}O_2$ and $LiNi_{0.5}Co_{0.5}O_2$, which have the same Δx. Among $LiNi_{1-y}Co_yO_2$ ($y=0.1$, 0.3 and 0.5) synthesized at 850 °C, $LiNi_{0.9}Co_{0.1}O_2$ has the largest intercalated Li quantity Δx, followed in order by $LiNi_{0.7}Co_{0.3}O_2$ and $LiNi_{0.5}Co_{0.5}O_2$.

$LiNi_{0.9}Co_{0.1}O_2$ shows the best intercalation and deintercalation reactions among $LiNi_{1-y}Co_yO_2$ ($y=0.1$, 0.3 and 0.5).

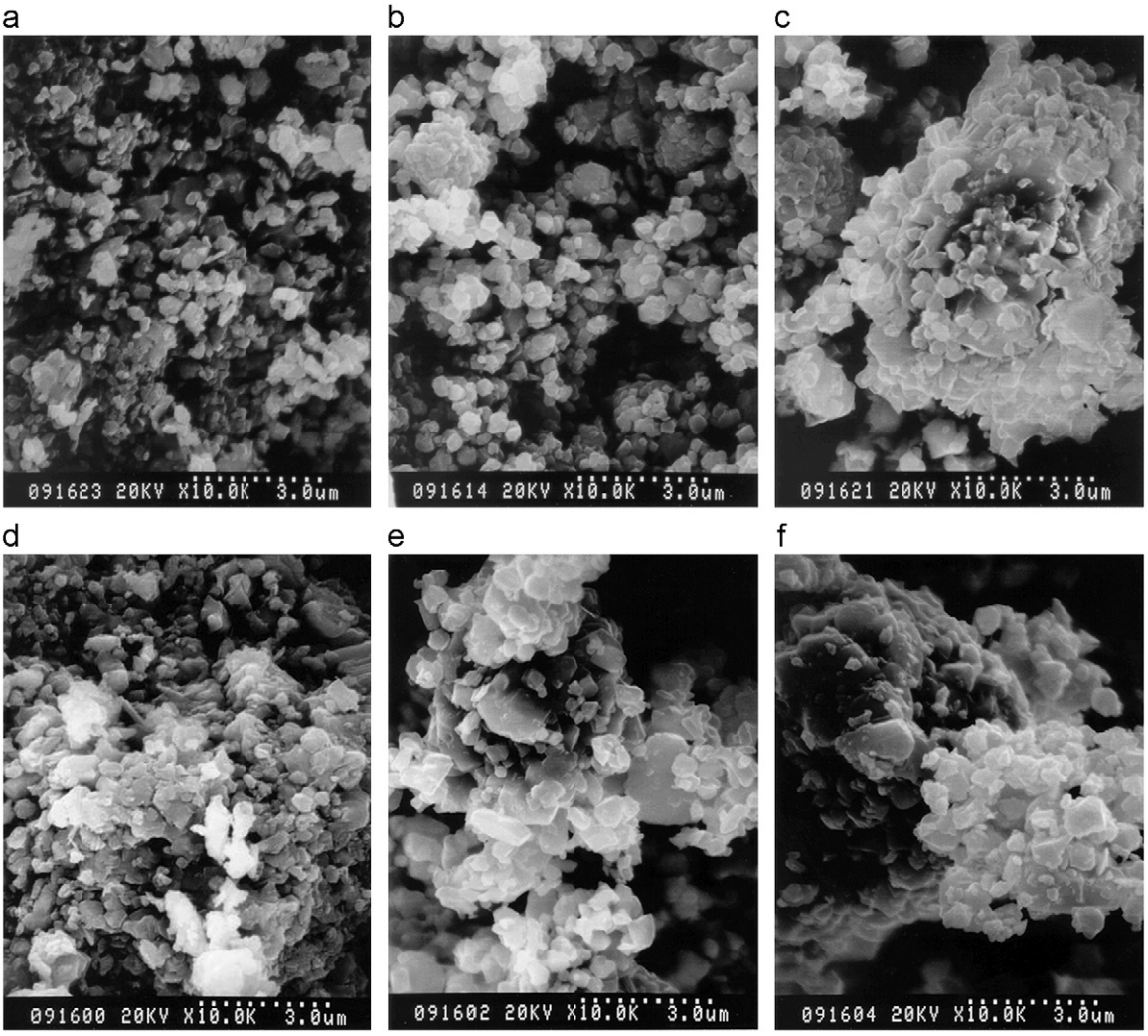

Fig. 3. SEM micrographs of $LiNi_{1-y}Co_yO_2$ synthesized from Li_2CO_3, $NiCO_3$ and Co_3O_4 at 800 °C; (a) $y=0.5$, (b) $y=0.3$, and (c) $y=0.1$, and at 850 °C; (d) $y=0.5$, (e) $y=0.3$, and (f) $y=0.1$.

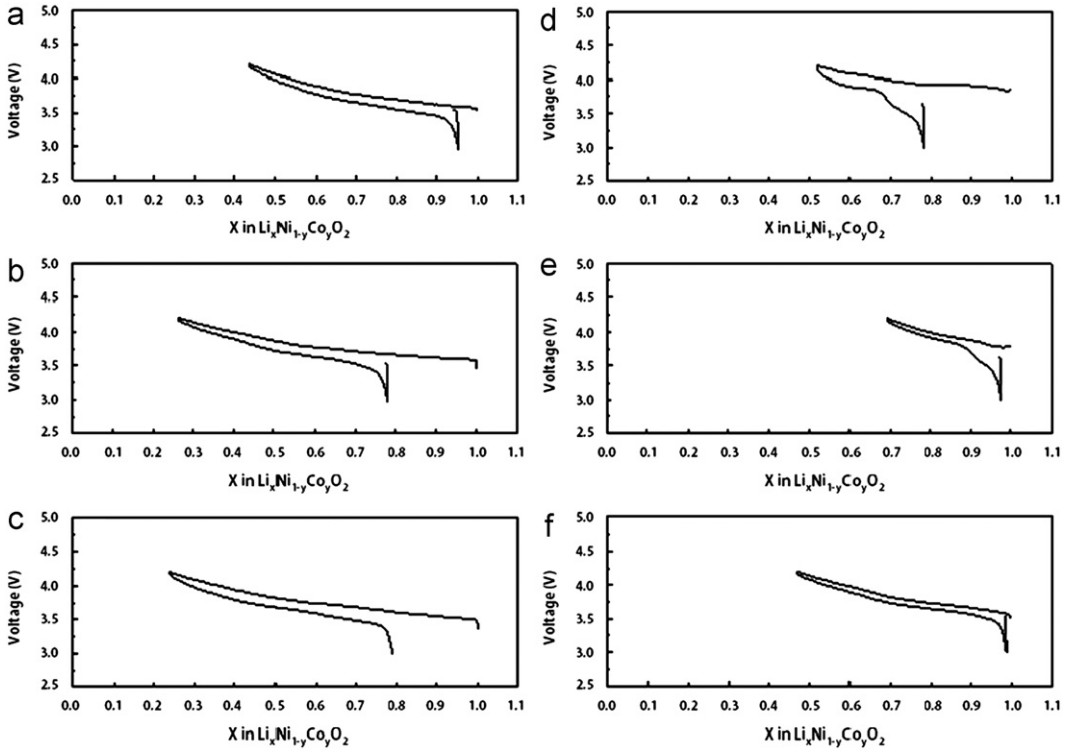

Fig. 4. Voltage vs. x in $Li_xNi_{1-y}Co_yO_2$ curves at a current density of 200 μA/cm^2 for the first charge–discharge cycle of $LiNi_{1-y}Co_yO_2$ synthesized at 800 °C; (a) y=0.5, (b) y=0.3, and (c) y=0.1, and at 850 °C; (d) y=0.5, (e) y=0.3, and (f) y=0.1.

Fig. 5 presents voltage vs. x in $Li_xNi_{1-y}Co_yO_2$ curves for the first and second charge–discharge cycles of $LiNi_{0.9}Co_{0.1}O_2$ synthesized at 800 °C and 850 °C. At the first cycle, $LiNi_{0.9}Co_{0.1}O_2$ synthesized at 800 °C has a larger value of intercalated Li quantity Δx than that synthesized at 850 °C. For the $LiNi_{0.9}Co_{0.1}O_2$ samples synthesized at 800 °C and 850 °C, the differences between the Δx values of the first and second cycles are equal. The polarization of $LiNi_{0.9}Co_{0.1}O_2$ sample synthesized at 850 °C is smaller than that of $LiNi_{0.9}Co_{0.1}O_2$ sample synthesized at 800 °C.

First charge capacities at a current density of 200 μA/cm^2 in the voltage range of 3.0–4.3 V for $LiNi_{1-y}Co_yO_2$ samples synthesized at 800 °C and at 850 °C are shown in Fig. 6. For a given composition, $LiNi_{1-y}Co_yO_2$ synthesized at 800 °C has a larger first discharge capacity than that synthesized at 850 °C, suggesting that the calcination at a higher temperature might cause more lithium loss. All of the $LiNi_{1-y}Co_yO_2$ (y=0.1, 0.3 and 0.5) samples synthesized at 800 °C have larger first discharge capacities than those synthesized at 850 °C. For $LiNi_{1-y}Co_yO_2$ (y=0.1, 0.3 and 0.5) samples synthesized at the same temperature, the first discharge capacity decreases as the Co content increases.

Fig. 7 presents the variations of the first charge capacity with y for $LiNi_{1-y}Co_yO_2$ synthesized at 800 °C and 850 °C. For $LiNi_{1-y}Co_yO_2$ (y=0.1, 0.3 and 0.5) synthesized at the same temperature, the first discharge capacity decreases as the Co content increases. $LiCoO_2$ has a theoretical discharge capacity of 274 mAh/g. However, Brandt [47] and Scrosati [48] reported that its practical discharge capacity is about 150 mAh/g since lithium ion is not deintercalated more than about 0.5 Li^+/mol due to structural stability problem. This is considered to lead to this result that the discharge capacity decreases as the Co content, y, increases. For a given composition, $LiNi_{1-y}Co_yO_2$ synthesized at 800 °C has a larger first discharge capacity than that synthesized at 850 °C, suggesting that the calcination at a higher temperature might cause more lithium loss. $LiNi_{0.9}Co_{0.1}O_2$ synthesized at 800 °C has the largest first discharge capacity (152 mAh/g), followed in order by $LiNi_{0.9}Co_{0.1}O_2$ synthesized at 850 °C (145 mAh/g), $LiNi_{0.7}Co_{0.3}O_2$ synthesized at 800 °C (142 mAh/g), $LiNi_{0.5}Co_{0.5}O_2$ synthesized at 800 °C (142 mAh/g), $LiNi_{0.7}Co_{0.3}O_2$ synthesized at 850 °C (78 mAh/g), and $LiNi_{0.5}Co_{0.5}O_2$ synthesized at 800 °C (72 mAh/g).

The variations of discharge capacity with number of cycles n for $LiNi_{1-y}Co_yO_2$ synthesized at 800 °C; (a) y=0.5, and (b) y=0.1, and at 850 °C; (c) y=0.5, (d) y=0.3, and (e) y=0.1 are shown in Fig. 8. The samples have quite good cycling performance except for $LiNi_{0.5}Co_{0.5}O_2$ synthesized at 800 °C. $LiNi_{0.9}Co_{0.1}O_2$ synthesized at 800 °C has the largest first discharge capacity (152 mAh/g) and quite good cycling performance with a discharge capacity of 146 mAh/g at n=5. It has a discharge capacity fading rate of 1.4 mAh/g/cycle. $LiNi_{0.9}Co_{0.1}O_2$ synthesized at 850 °C has secondarily the largest first discharge capacity (145 mAh/g), and a discharge capacity of 132 mAh/g at n=5 with a discharge capacity fading rate of 3.2 mAh/g/cycle. The $LiNi_{0.9}Co_{0.1}O_2$ samples synthesized at 800 °C and 850 °C seem to have similar cycling stabilities, but $LiNi_{0.9}Co_{0.1}O_2$ synthesized at

800 °C has a little better cycling stability than $LiNi_{0.9}Co_{0.1}O_2$ synthesized at 850 °C. As mentioned above, Kang et al. [39] investigated the structure and electrochemical properties of the $Li_xCo_yNi_{1-y}O_2$ (y=0.1, 0.3, 0.5, 0.7 and 1.0) system synthesized by a solid-state reaction with various starting materials to optimize the characteristics and synthetic conditions of the $Li_xCo_yNi_{1-y}O_2$. The first discharge capacities of $Li_xCo_yNi_{1-y}O_2$ were 60–180 mAh/g, depending on synthesis conditions. $LiCo_yNi_{1-y}O_2$ samples were synthesized at 800 °C and 850 °C, by the solid-state reaction method, using the starting materials $LiOH \cdot H_2O$ or Li_2CO_3, NiO or $NiCO_3$, and Co_3O_4 or $CoCO_3$ [46]. The $LiNi_{0.7}Co_{0.3}O_2$ synthesized at 800 °C using $LiOH \cdot H_2O$, NiO and Co_3O_4 exhibited a larger first discharge capacity of 162 mAh/g than the other samples. $LiNi_{0.9}Co_{0.1}O_2$ synthesized at 850 °C using Li_2CO_3, NiO and Co_3O_4 showed excellent cycling performance. $LiNi_{0.9}Co_{0.1}O_2$ synthesized at 800 °C in this work had the largest first discharge capacity (152 mAh/g), which is lower than those of the above reported results, but had quite good cycling performance.

The voltage vs. x in $Li_xNi_{1-y}Co_yO_2$ curves at a current density of 200 μA/cm^2 for the first charge–discharge cycle of $LiNi_{1-y}Co_yO_2$ in Figs. 4 and 5 show that, as compared with the quantity of the deintercalated Li ions by the first charging, that of the intercalated Li ions by the first discharging is much smaller, which is revealed by the

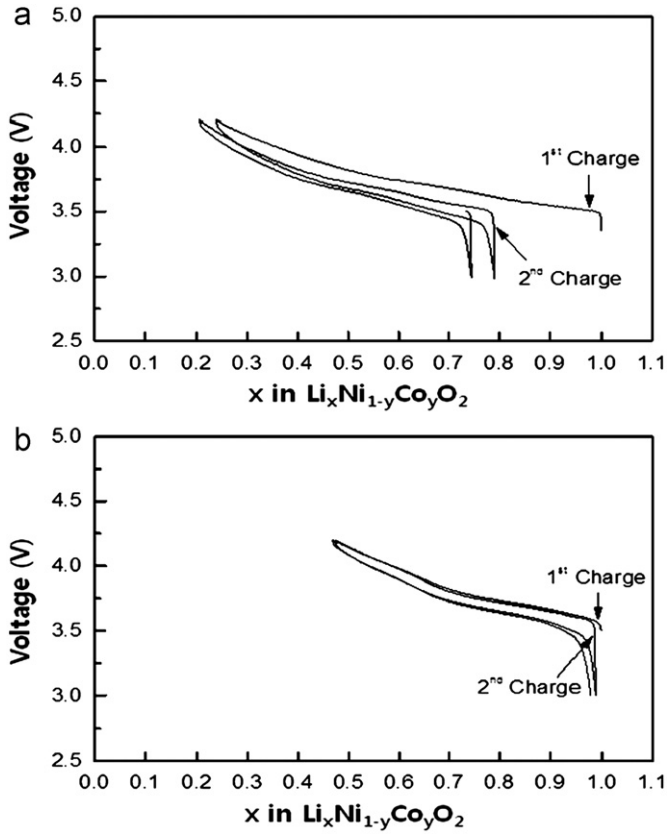

Fig. 5. Voltage vs. x in $Li_xNi_{1-y}Co_yO_2$ curves for the first and second charge–discharge cycles of $LiNi_{0.9}Co_{0.1}O_2$ synthesized (a) at 800 °C, and (b) at 850 °C.

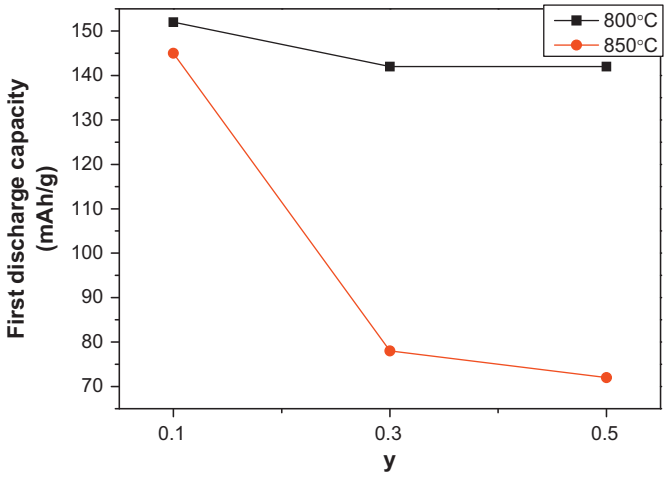

Fig. 7. Variations of the first discharge capacity with y for $LiNi_{1-y}Co_yO_2$ synthesized at 800 °C and 850 °C.

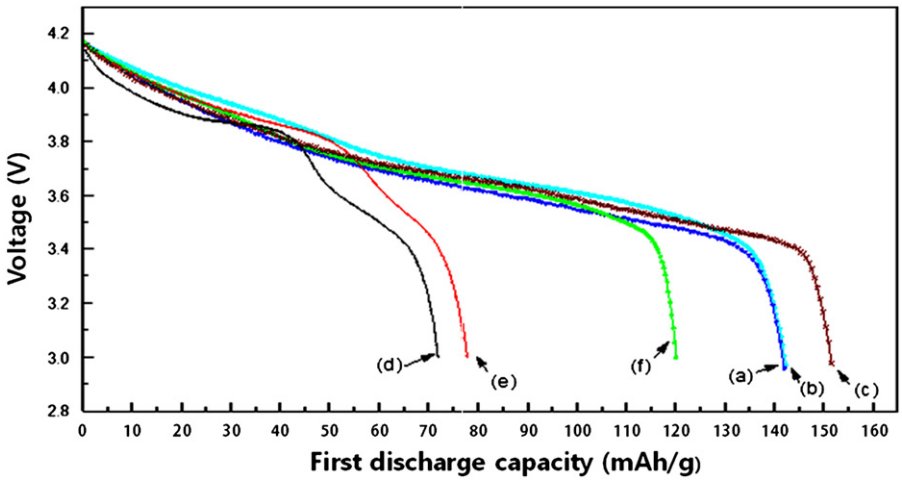

Fig. 6. First discharge capacities at a current density of 200 μA/cm^2 in the voltage range of 3.0–4.3 V for $LiNi_{1-y}Co_yO_2$ synthesized at 800 °C; (a) y=0.5, (b) y=0.3, and (c) y=0.1, and at 850 °C; (d) y=0.5, (e) y=0.3, and (f) y=0.1.

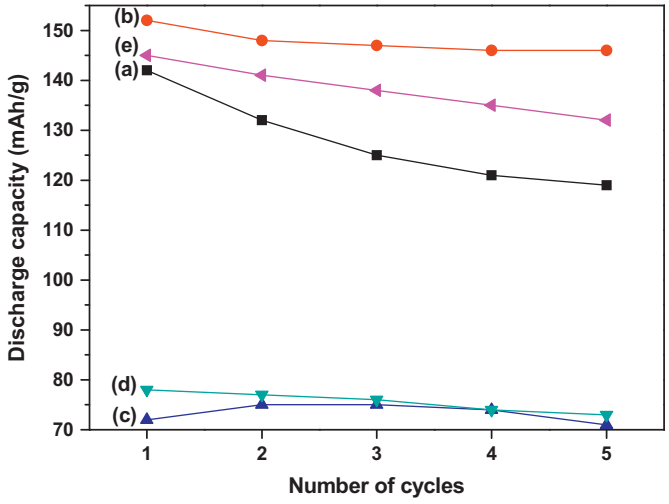

Fig. 8. Variations of discharge capacity with number of cycles n for $LiNi_{1-y}Co_yO_2$ synthesized at 800 °C; (a) $y=0.5$, and (b) $y=0.1$, and at 850 °C; (c) $y=0.5$, (d) $y=0.3$, and (e) $y=0.1$.

difference in Δx of the first charge and discharge curves, for all the samples. The lengths of the plateaus in the charge and discharge curves are proportional to the charge and discharge capacities, respectively. During the first charging, Li ions deintercalate not only from stable 3b sites but also from unstable 3b sites. After deintercalation from the unstable 3b sites, the unstable 3b sites will be destroyed. This is considered to be the reason for the smaller quantity of the intercalated Li ions by the first discharging than that of the deintercalated Li ions by the first charging.

The voltage vs. x in $Li_xNi_{1-y}Co_yO_2$ curves for the first and second charge–discharge cycles of $LiNi_{0.7}Co_{0.3}O_2$ synthesized at 800 °C, and at 850 °C in Fig. 5 show that the difference between Δx values of the second charge and discharge curves is smaller than that of the first charge and discharge curves. This shows that destruction of unstable 3b sites occurs less severely at the second cycle than at the first cycle.

In the voltage vs. x in $Li_xNi_{1-y}Co_yO_2$ curves for the first and second charge–discharge cycles of $LiNi_{0.9}Co_{0.1}O_2$ synthesized at 800 °C and 850 °C in Fig. 5, the charge–discharge curves exhibit quite long plateaus, where two phases co-exist [49]. Arai et al. [50] reported that, during charging and discharging, $LiNiO_2$ goes through three phase transitions; the phase transitions from a hexagonal structure (H1) to a monoclinic structure (M), from a monoclinic structure (M) to a second hexagonal structure (H2), and from the second hexagonal structure (H2) to a third hexagonal structure (H3) or vice versa. Ohzuku et al. [40] reported that, during charging and discharging, $LiNiO_2$ goes through four phase transitions; the phase transitions from H1 to M, from M to H2, from H2 to hexagonal structures H2+H3, and from H2+H3 to H3 or vice versa. Song et al. [51] reported that $-dx/|dV|$ vs. V curves of $LiNi_{1-y}Ti_yO_2$ ($y=0.012$ and 0.025) for charging and discharging showed four peaks, revealing four phase transitions from H1 to M, from M to H2, from H2 to H2+H3, and from H2+H3 to H3 or vice versa.

4. Conclusions

When the particle sizes were compared for the samples synthesized at the same temperature, particle size increased very slowly as the Co content decreased, but that size was overall quite similar. The $LiNi_{1-y}Co_yO_2$ ($y=0.1$, 0.3 and 0.5) samples synthesized at 800 °C and $LiNi_{0.9}Co_{0.1}O_2$ synthesized at 850 °C exhibited quite small polarization. When the first discharge capacities of $LiNi_{1-y}Co_yO_2$ ($y=0.1$, 0.3 and 0.5) synthesized at each temperature were compared, the first discharge capacity decreased as the Co content increased. $LiNi_{0.9}Co_{0.1}O_2$ synthesized at 800 °C had the largest first discharge capacity (152 mAh/g) and quite good cycling performance, with a discharge capacity fading rate of 1.4 mAh/g/cycle.

References

[1] K. Ozawa, Lithium-ion rechargeable batteries with $LiCoO_2$ and carbon electrodes: the $LiCoO_2$/C system, Solid State Ionics 69 (1994) 212–221.
[2] R. Alcántara, P. Lavela, J.L. Tirado, R. Stoyanova, E. Zhecheva, Structure and electrochemical properties of boron-doped $LiCoO_2$, Journal of Solid State Chemistry 134 (1997) 265–273.
[3] Z.S. Peng, C.R. Wan, C.Y. Jiang, Synthesis by sol–gel process and characterization of $LiCoO_2$ cathode materials, Journal of Power Sources 72 (1998) 215–220.
[4] W.D. Yang, C.Y. Hsieh, H.J. Chuang, Y.S. Chen, Preparation and characterization of nanometric-sized $LiCoO_2$ cathode materials for lithium batteries by a novel sol–gel method, Ceramics International 36 (1) (2010) 135–140.
[5] S.K. Kim, D.H. Yang, J.S. Sohn, Y.C. Jung, Resynthesis of $LiCo_{1-x}Mn_xO_2$ as a cathode material for lithium secondary batteries, Metals and Materials International 18 (2) (2012) 321–326.
[6] J.R. Dahn, U. von Sacken, C.A. Michal, Structure and electrochemistry of $Li_{1\pm y}NiO_2$ and a new Li_2NiO_2 phase with the $Ni(OH)_2$ structure, Solid State Ionics 44 (1990) 87–97.
[7] J.R. Dahn, U. von Sacken, M.W. Juzkow, H. Al-Janaby, Rechargeable $LiNiO_2$/carbon cells, Journal of the Electrochemical Society 138 (1991) 2207–2212.
[8] H.U. Kim, D.R. Mumm, H.R. Park, M.Y. Song, Synthesis by a simple combustion method and electrochemical properties of $LiCo_{1/3}Ni_{1/3}Mn_{1/3}O_2$, Electronic Materials Letters 6 (3) (2010) 91–95.
[9] S.H. Ju, J.H. Kim, Y.C. Kang, Electrochemical properties of $LiNi_{0.8}Co_{0.2-x}Al_xO_2$ ($0 \le x \le 0.1$) cathode particles prepared by spray pyrolysis from the spray solutions with and without organic additives, Metals and Materials International 16 (2) (2010) 299–303.
[10] D.H. Kim, Y.U. Jeong, D.H. Kim, Y.U. Jeong, Crystal structures and electrochemical properties of $LiNi_{1-x}Mg_xO_2$ ($0 \le x \le 0.1$) for cathode materials of secondary lithium batteries, Journal of the Korean Institute of Metals and Materials 48 (3) (2010) 262–267.
[11] S.N. Kwon, J.H. Song, D.R. Mumm, Effects of cathode fabrication conditions and cycling on the electrochemical performance of $LiNiO_2$ synthesized by combustion and calcination, Ceramics International 37 (5) (2011) 1543–1548.
[12] M.Y. Song, C.K. Park, H.R. Park, D.R. Mumm, Variations in the electrochemical properties of metallic elements-substituted $LiNiO_2$ cathodes with preparation and cathode fabrication conditions, Electronic Materials Letters 8 (1) (2012) 37–42.
[13] M.Y. Song, D.R. Mumm, C.K. Park, H.R. Park, Cycling performances of $LiNi_{1-y}M_yO_2$ (M=Ni, Ga, Al and/or Ti) synthesized by

wet milling and solid-state method, Metals and Materials International 18 (3) (2012) 465–472.
[14] J.M. Tarascon, E. Wang, F.K. Shokoohi, W.R. Mckinnon, S. Colson, The spinel phase of $LiMn_2O_4$ as a cathode in secondary lithium cells, Journal of the Electrochemical Society 138 (1991) 2859–2864.
[15] A.R. Armstrong, P.G. Bruce, Synthesis of layered $LiMnO_2$ as an electrode for rechargeable lithium batteries, Letters in Nature 381 (1996) 499–500.
[16] M.Y. Song, D.S. Ahn, On the capacity deterioration of Spinel phase $LiMn_2O_4$ with cycling around 4V, Solid State Ionics 112 (1998) 21–24.
[17] M.Y. Song, D.S. Ahn, H.R. Park, Capacity fading of spinel phase $LiMn_2O_4$ with cycling, Journal of Power Sources 83 (1999) 57–60.
[18] D.S. Ahn, M.Y. Song, Variations of the electrochemica properties of $LiMn_2O_4$ with synthesis conditions, Journal of the Electrochemical Society 147 (3) (2000) 874–879.
[19] H.J. Guo, Q.H. Li, X.H. Li, Z.X. Wang, W.J. Peng, Novel synthesis of $LiMn_2O_4$ with large tap density by oxidation of manganese powder, Energy Conversion and Management 52 (4) (2011) 2009–2014.
[20] C. Wan, M. Cheng, D. Wu, Synthesis of spherical spinel $LiMn_2O_4$ with commercial manganese carbonate, Powder Technology 210 (1) (2011) 47–51.
[21] J.W. Park, J.H. Yu, K.W. Kim, H.S. Ryu, J.H. Ahn, C.S. Jin, K.H. Shin, Y.C. Kim, H.J. Ahn, Surface morphology changes of lithium/sulfur battery using multi-walled carbon nanotube added sulfur electrode during cyclings, Journal of the Korean Institute of Metals and Materials 49 (2) (2011) 174–179.
[22] Y. Nishida, K. Nakane, T. Satoh, Synthesis and properties of gallium-doped $LiNiO_2$ as the cathode material for lithium secondary batteries, Journal of Power Sources 68 (1997) 561–564.
[23] P. Barboux, J.M. Tarascon, F.K. Shokoohi, The use of acetates as precursors for the low-temperature synthesis of $LiMn_2O_4$ and $LiCoO_2$ intercalation compounds, Journal of Solid State Chemistry 94 (1991) 185–196.
[24] J. Morales, C. Perez-Vicente, J.L. Tirado, Cation distribution and chemical deintercalation of $Li_{1-x}Ni_{1+x}O_2$, Materials Research Bulletin 25 (1990) 623–630.
[25] A. Rougier, I. Saadoune, P. Gravereau, P. Willmann, C. Delmas, Effect of cobalt substitution on cationic distribution in $LiNi_{1-y}Co_yO_2$ electrode materials, Solid State Ionics 90 (1996) 83–90.
[26] B.J. Neudecker, R.A. Zuhr, B.S. Kwak, J.B. Bates, J.D. Robertson, Lithium manganese nickel oxides $Li_x(Mn_yNi_{1-y})_{2-x}O_2$, Journal of the Electrochemical Society 145 (1998) 4148–4157.
[27] C. Delmas, I. Saadoune, Electrochemical and physical properties of the $Li_xNi_{1-y}Co_yO_2$ phases, Solid State Ionics 53–56 (1992) 370–375.
[28] E. Zhecheva, R. Stoyanova, Stabilization of the layered crystal structure of $LiNiO_2$ by Co-substitution, Solid State Ionics 66 (1993) 143–149.
[29] C. Delmas, I. Saadoune, A. Rougier, The cycling properties of the $Li_xNi_{1-y}Co_yO_2$ electrode, Journal of Power Sources 43–44 (1993) 595–602.
[30] A. Ueda, T. Ohzuku, Solid-state redox reactions of $LiNi_{1/2}Co_{1/2}O_2$ ($R\bar{3}$ m) for 4 V secondary lithium cells, Journal of the Electrochemical Society 141 (1994) 2010–2014.
[31] M. Menetrier, A. Rougier, C. Delmas, Cobalt segregation in the $LiNi_{1-y}Co_yO_2$ solid solution: A preliminary ^7Li NMR study, Solid State Communications 90 (1994) 439–442.
[32] R. Alcantara, J. Morales, J.L. Tirado, R. Stoyanova, E. Zhecheva, Structure and electrochemical properties of $Li_{1-x}(Ni_yCo_{1-y})_{1+x}O_2$ Effect of chemical delithiation at 0 °C, Journal of the Electrochemical Society 142 (1995) 3997–4005.
[33] B. Banov, J. Bourilkov, M. Mladenov, Cobalt stabilized layered lithium–nickel oxides, cathodes in lithium rechargeable cells, Journal of Power Sources 54 (1995) 268–270.
[34] Y.M. Choi, S.I. Pyun, S.I. Moon, Effects of cation mixing on the electrochemical lithium intercalation reaction into porous $Li_{1-\delta}Ni_{1-y}Co_yO_2$ electrodes, Solid State Ionics 89 (1996) 43–52.
[35] S.J. Lee, J.K. Lee, D.W. Kim, H.K. Baik, S.M. Lee, Fabrication of thin film $LiCo_{0.5}Ni_{0.5}O_2$ cathode for Li rechargeable microbattery, Journal of the Electrochemical Society 143 (1996) L268–L270.
[36] D. Caurant, N. Baffier, B. Garcia, J.P. Pereira-Ramos, Synthesis by a soft chemistry route and characterization of $LiNi_xCo_{1-x}O_2$ ($0 \le x \le 1$) cathode materials, Solid State Ionics 91 (1996) 45–54.
[37] K. Amine, H. Yasuda, Y. Fujita, New process for low temperature preparation of $LiNi_{1-x}Co_xO_2$ Cathode material for lithium cells, Annales de Chimie Science des Materiaux 23 (1998) 37–42.
[38] C.C. Chang, N. Scarr, P.N. Kumta, Synthesis and electrochemical characterization of $LiMO_2$ (M = Ni, $Ni_{0.75}Co_{0.25}$) for rechargeable lithium ion batteries, Solid State Ionics 112 (1998) 329–344.
[39] S.G. Kang, K.S. Ryu, S.H. Chang, S.C. Park, The novel synthetic route to $LiCo_yNi_{1-y}O_2$ as a cathode material in lithium secondary batteries, Bulletin of the Korean Chemical Society 22 (12) (2001) 1328–1332.
[40] T. Ohzuku, A. Ueda, M. Nagayama, Electrochemistry and structural chemistry of $LiNiO_2$ ($R\bar{3}$ m) for 4 V secondary lithium cells, Journal of the Electrochemical Society 140 (1993) 1862–1870.
[41] Z. Lu, X. Huang, H. Haung, L. Chen, J. Schoonman, The phase transition and optimal synthesis temperature of $LiNiO_2$, Solid State Ionics 120 (1999) 103–107.
[42] M. Guilmard, A. Rougier, M. Grune, L. Croguennec, C. Delmas, Effects of aluminum on the structural and electrochemical properties of $LiNiO_2$, Journal of Power Sources 115 (2003) 305–314.
[43] B.J. Hwang, R. Santhanam, C.H. Chen, Effect of synthesis conditions on electrochemical properties of $LiCo_yNi_{1-y}O_2$ cathode for lithium rechargeable batteries, Journal of Power Sources 114 (2003) 244–252.
[44] S.H. Park, C.S. Yoon, S.G. Kang, H.S. Kim, S.I. Moon, Y.K. Sun, Synthesis and structural characterization of layered Li $[Ni_{1/3}Co_{1/3}Mn_{1/3}]O_2$ cathode materials by ultrasonic spray pyrolysis method, Electrochimica Acta 49 (2004) 557–563.
[45] B.H. Kim, J.H. Kim, I.H. Kwon, M.Y. Song, Electrochemical properties of $LiNiO_2$ cathode material synthesized by the emulsion method, Ceramics International 33 (2007) 837–841.
[46] M.Y. Song, H. Rim, E. Bang, Electrochemical properties of cathode materials $LiNi_{1-y}Co_yO_2$ synthesized using various starting materials, Journal of Applied Electrochemistry 34 (2004) 383–389.
[47] K. Brandt, Historical development of secondary lithium batteries, Solid State Ionics 69 (3-4) (1994) 173–183.
[48] B. Scrosati, Lithium rocking chair batteries: An old concept?, Journal of the Electrochemical Society 139 (1992) 2776–2781.
[49] W. Li, J.N. Reimers, J.R. Dahn, In situ x-ray diffraction and electrochemical studies of $Li_{1-x}NiO_2$, Solid State Ionics 67 (1993) 123–130.
[50] H. Arai, S. Okada, H. Ohtsuka, M. Ichimura, J. Yamaki, Characterization and cathode performance of $Li_{1-x}Ni_{1+x}O_2$ prepared with the excess lithium method, Solid State Ionics 80 (1995) 261–269.
[51] M.Y. Song, D.S. Lee, H.R. Park, Electrochemical properties of $LiNi_{1-y}Ti_yO_2$ and $LiNi_{0.975}M_{0.025}O_2$ (M = Zn, Al, and Ti) synthesized by the solid-state reaction method, Materials Research Bulletin 47 (2012) 1021–1027.